*Journal of Imaging Science and Technology*® 56(1): 010503-1–010503-10, 2012.


# New Minutiae-Matching Method Based on Partial Fingerprints

**Chin-Hsin Chang, Jin-Hong Lin, and Innchyn Her**
*Department of Electro-Mechanical Engineering, National Sun Yat-sen University Kaohsiung, 70, Lienhai Rd., Kaohsiung 80424, Taiwan*
*E-mail: d973020011@student.nsysu.edu.tw*

**Abstract.** *As information technologies have advanced greatly in the recent years, the security problem of information networks becomes all the more important. As a result, biometric identification techniques have been given considerable attention. Fingerprint-related techniques, due to their desirable properties, e.g., universality, perpetuity, collectability, and particularity, are most widely applied and documented. However, in practice, collected fingerprint images are not always of good shape. They often are noisy or contain only partial fingerprints. Therefore, in this article, the authors propose a partial fingerprint comparison technique, called the triangular scheme, to combine with a coefficient of orientation deflection variation and other advancements, to obtain satisfactory matching based on only partial fingerprints. By the proposed scheme, they show that within a wide range of average reliability when the test image and a database image could have only five matched minutia points, the authors have both fault resistance rate and fault acceptance rate error values down to 29%, and the total matching accuracy reaches 71%. © 2012 Society for Imaging Science and Technology.*
[DOI: xxx ]

## INTRODUCTION

In 1788, Mayer noticed that it was nearly impossible for any two persons to have identical fingerprints. Based on his suggestion and other related works of contemporary researchers, Henry presented,[1] roughly at the turn of the 20th century, the framework of modern fingerprint identification theories.

A fingerprint consists of, in general, ridges and valleys. These are the fundamental features used in forensic identification. A fingerprint often also has cores or deltas, as shown in Figure 1(a), and they can be used as additional matching criteria. Besides the cores and the deltas, the patterns that compose the major part of a fingerprint are called the minutiae. A minutiae point is then defined where a bifurcation or an ending occurs along a ridge, as shown in Fig. 1(b). Figure 2(a) shows the standard procedure of an automated fingerprint identification system (AFIS) as proposed by Jain et al.[2] in 1997.

This article is about a minutiae-matching method developed specially for the identification of partial fingerprints, e.g., the one in Fig. 2(b). This scheme includes using frequency-based properties for minutiae searching and selection, and a new coefficient of orientation deflection variance as an image feature for fingerprint matching. Some pertinent background techniques are reviewed before proposed approach is discussed. The proposed scheme is verified in this article with degraded fingerprint images from the fingerprint verification competition (FVC) database.

Received Feb. 3, 2011; accepted for publication Nov. 7, 2011; published online Mar. 21, 2012
1062-3701/2012/56(1)/010503/10/$20.00.

## PREPROCESSING AND POSTPROCESSING

Figure 3(a) illustrates commonly used preprocessing steps for a fingerprint verification system. Among them, normalization, histogram equalization, and thinning algorithms have become standard material in textbooks and many papers regarding image processing.[3–5] A fingerprint image after both normalization and histogram equalization is shown in Fig. 3(b).

## ORIENTATION FIELD

The orientation of the ridges in a fingerprint is a crucial feature for its verification. To calculate the orientation field in an image, gradient methods,[6–8] filter methods,[9–11] and zero-pole methods are commonly used.[12–14] The gradient methods are more popular, and in this article we combine the ideas given by Hong et al.[3] and Kass and Witkin.[6] After applying histogram equalization to a fingerprint image, we compute

$$\begin{aligned} J_x(i,j) &= G_x(i,j)^2 - G_y(i,j)^2, \\ J_y(i,j) &= 2G_x(i,j)G_y(i,j), \end{aligned} \tag{1}$$

$$\begin{aligned} J'_x(i,j) &= \sum_{u=1}^{M}\sum_{v=1}^{N} J_x(u,v), \\ J'_y(i,j) &= \sum_{u=1}^{M}\sum_{v=1}^{N} J_y(u,v), \end{aligned} \tag{2}$$

$$\theta(i,j) = \frac{1}{2}\tan^{-1}\left(\frac{J'_y(i,j)}{J'_x(i,j)}\right), \tag{3}$$

where $J_x(i, j)$ and $J_y(i, j)$ are the two axial components of the square gradient at image point $(i, j)$, while $G_x(i, j)$ and $G_y(i, j)$ are the gradients, respectively. These quantities are computed using Sobel operators.[5] Using these equations,

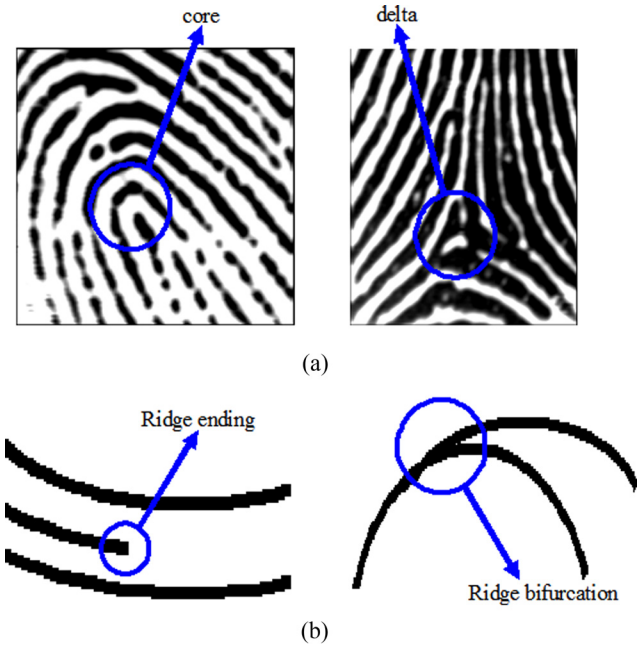


Figure 1. Schematics of fingerprint features: (a) fundamental features of the fingerprints (b) minutiae points of the fingerprints.

we can calculate the principle orientation $\theta(i, j)$ for any $M \times N$ image block. Practically, it is advisable to use $8 \times 8$ (64 pixels) image blocks, as in this article.

A fingerprint image may not always be crisp and clear. There can be all kinds of noise, which result in inaccurate orientation computation for affected image blocks. In this article, we use a low-pass filter to allay the influence of noises.[5] A sample result image is shown in Fig. 3(b).

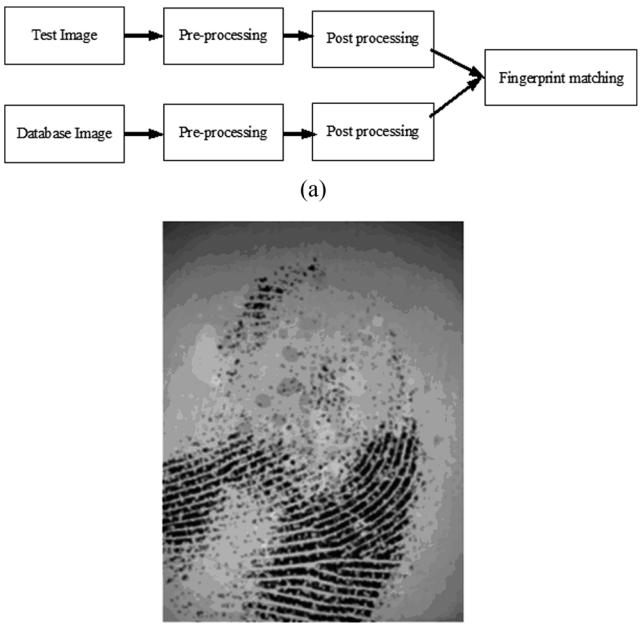


Figure 2. AFIS flowchart and a partial fingerprint: (a) the AFIS proposed by Jain[2] (b) a partial fingerprint.

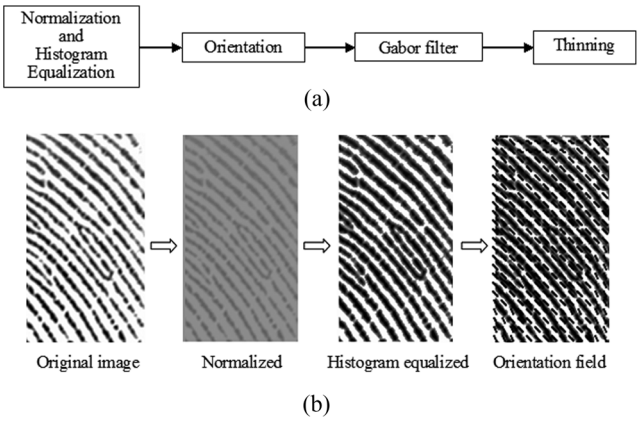


Figure 3. Fingerprint preprocessing steps: (a) flowchart of preprocessing steps (b) a fingerprint under pre-processing.

## GABOR FILTER

The Gabor filter has long been used for image outline analysis due to many desirable characteristics. This article uses the procedure given by Hong et al.[3] and follows the guideline by Xiao and Peng[15] to select the region of filter frequency for images.

Let an even Gabor filter function be represented as

$$G(x, y, q_k, f) = \exp\left\{-\frac{1}{2}\left[\frac{(x')^2}{\sigma_x^2} + \frac{(y')^2}{\sigma_y^2}\right]\right\} \cos[2\pi(x')f],$$
$$x' = x\cos\theta_k + y\sin\theta_k,$$
$$y' = -x\sin\theta_k + y\cos\theta_k. \quad (4)$$

From the above equations, we know that we need to choose proper orientation $\theta_k$ and a frequency $f$ for Gabor filter. The orientation part is easier, for we have already discussed that in the "Orientation Field" section. As for selecting the frequency, see Figure 4(a).

Let, an $N \times N$ image area is used to compute the orientation of the ridges, in this research, we enlarge this area of interest to an $N \times 3N$ (denoted as h × w in Fig. 4) rectangle, and rotate it to align the orientation of the ridges, so as to more accurately compute the repeating frequency of the ridges. Here, relevant geometric transformation techniques are used for the rotation of the image block.[16]

Subsequently, we compute $Z$ that is the gap between two adjacent peaks in Fig. 4(a). By Xiao's algorithm,[15] $Z$ is bounded below by $T_1$ and above by $T_2$, i.e. $T_1 < Z < T_2$ to facilitate calculation. The bounds are determined beforehand when a set of test fingerprint images are selected. In this article, $T_1 = 3$ and $T_2 = 8$. Knowing $Z$, we can regard its reciprocal as a crude frequency $f$ for the block. In this article, however, a filter is used for obtaining a more reliable frequency $F(i, j)$. This is shown in the following total Gabor computations:

$$F(i,j) = \frac{1}{w_\Omega^2} \sum_{u=-\frac{w_\Omega}{2}}^{u=\frac{w_\Omega}{2}} \sum_{v=-\frac{w_\Omega}{2}}^{v=\frac{w_\Omega}{2}} f(i-u, j-v), \quad (5)$$

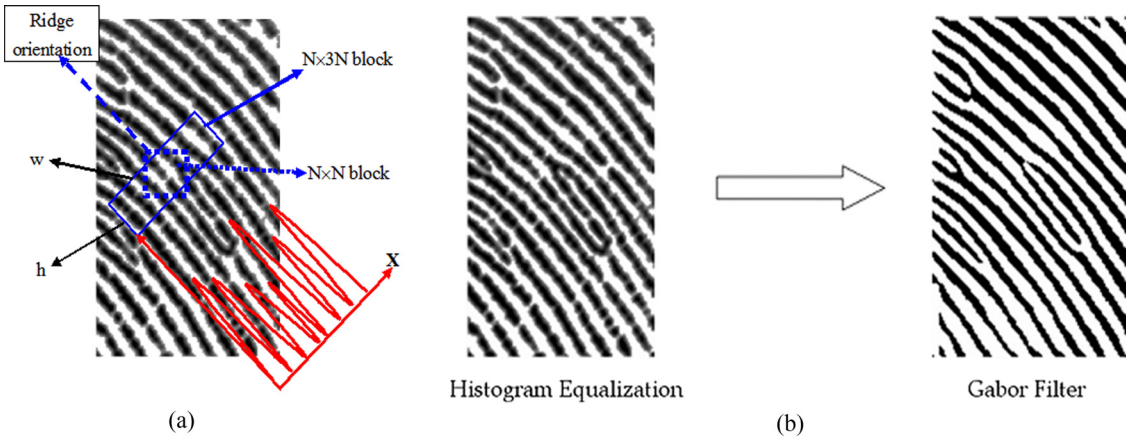


Figure 4. Fingerprint frequency and Gabor filtering: (a) frequency computation of a fingerprint (b) effect of Gabor filter.

$$E(i,j) = \sum_{u=-\frac{w_g}{2}}^{\frac{w_g}{2}} \sum_{v=-\frac{w_g}{2}}^{\frac{w_g}{2}} G(u,v,O(i,j),F(i,j))H(i-u,j-v), \tag{6}$$

$$E(i,j) = \begin{cases} 0 & \text{if } E(i,j) \le T_k \\ 255 & \text{otherwise} \end{cases}. \tag{7}$$

In the above equation, $H(i, j)$ is the input image and $E(i, j)$ is the output image. The blur filter $(w_\Omega \times w_\Omega)$, in this example contains $7 \times 7 = 49$ pixels, while the Gabor filter $(w_g \times w_g)$ contains $11 \times 11 = 121$ pixels. The results are shown in Fig. 4(b), where $T_k$ is set to the peak value of 255.

## MINUTIAE EXTRACTION

The enhanced minutiae extraction scheme used in article is partly based on a method proposed by Tico and Kuosmanen.[17] First, candidate minutiae points are labeled by checking all $3 \times 3$ blocks in the input image. Then, an $n \times n$ mask is defined on each candidate minutiae point, as in Figure 5(a), with such point being labeled as $(-1)$ in the center. Traveling around the perimeter of the mask, we register all minutiae points (labeled as 1) encountered, and denote the count as $C$. Then, as illustrated in Fig. 5(a), $C = 1$ corresponds with a real ridge ending and $C = 3$ corresponds with a real ridge bifurcation.

In our experiments, we notice that there is a need to refine the above method, mainly to avoid the occurrence of so-called false minutiae points. As in Fig. 5(b), when a minutia is found, we double-check its validity by constructing another $m \times m$ mask around it, where m is chosen according to the size of the test image. When going around the perimeter of the second mask, if the color of the pixels (as in Fig. 5) changes from white to black more than one time on any side, then the minutiae point in center is a false minutia and should be discarded.

## MINUTIAE MATCHING

There are largely three types of fingerprint matching methods: Gabor type methods,[11] minutiae matching methods,[18–20] and those assisted by Hough transforms.[21–23] An issue often discussed is the balance between accuracy and speed. Apart from the many existing methods in the literature,[24,25] we propose a matching scheme specialized for partial fingerprints. It is called the triangular matching scheme and the following are its main steps:

### *Locating Correlative Points*

We start with a search of possible correlative points, which collectively mark the relationship between the test image and a database image. For any partial fingerprint test image, e.g., Figure 6(a), let a minutia point is known to be located at $(i, j)$. The frequency $f_1(i, j)$ of the $w_f \times w_f$ block around $(i, j)$ can be obtained by the above-stated method. Besides, we also calculate the frequency of the eight neighboring $w_f \times w_f$ blocks. (We use subscript 1 to denote the block at the center.) Thus, we have a total of nine frequency samples associated with each minutiae point in the test image, and we do the same for the database image.

Now, let $n$ and $m$ be the numbers of minutiae points found in the partial fingerprint image and the database fingerprint image, respectively. First, we want to have

$$\left| f_1(i,j) - f'_1(i'_m, j'_m) \right| \le T_3, \tag{8}$$

where $f'_1(i'_m, j'_m)$ is the frequency around some minutiae point in the database fingerprint image to be compared. $T_3$ is a threshold value determined according to the database used. If the above criterion is not met, simply skip to another minutiae point in the database image.

However, even though for some pair of minutiae points the above equation holds, they do not guarantee to be correctly related. We need to make use of all the neighboring frequency values $f_s(i_n, j_n)$, $s = 2$ to 9. Therefore, if the total count of the minutiae points that satisfy the above equation is $a$, then, we have

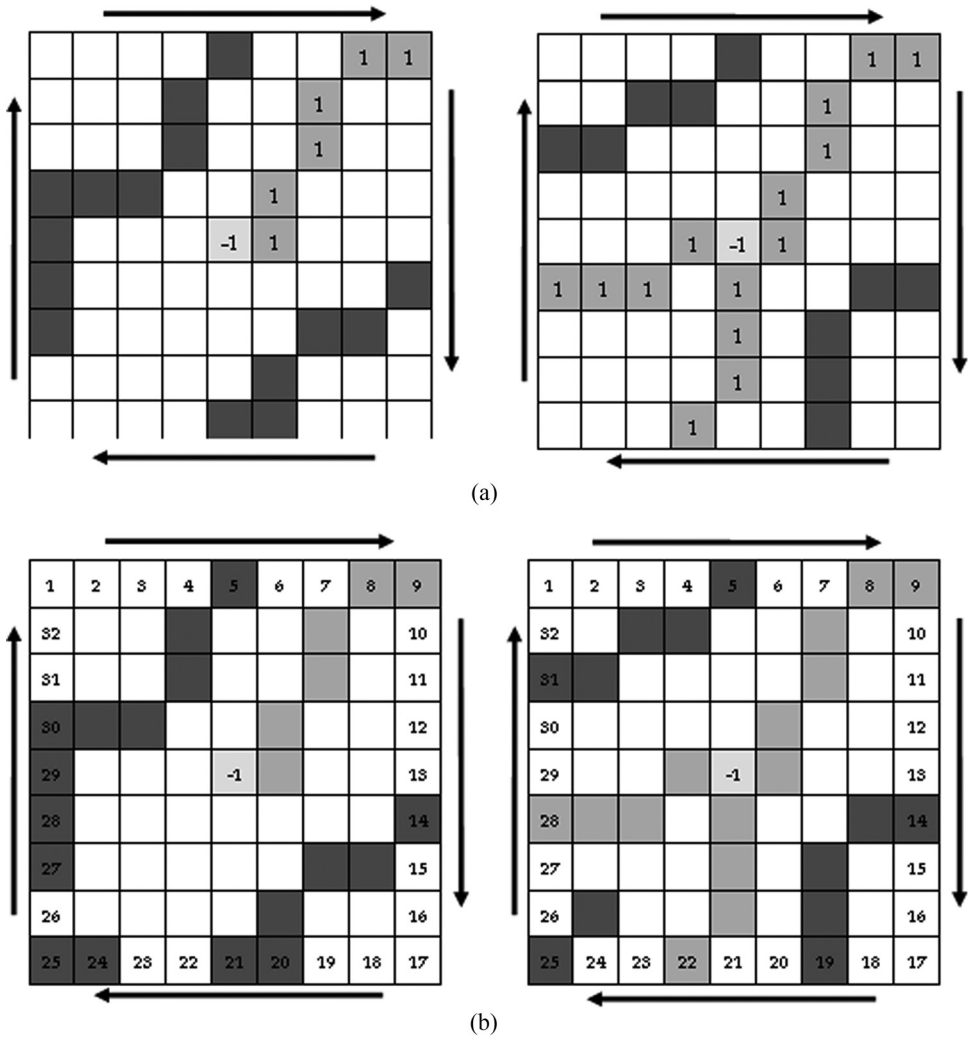


Figure 5. Minutiae extraction and refinement: (a) using an $n \times n$ mask around a candidate minutia (b) the use of an m×m mask for removing false minutia.

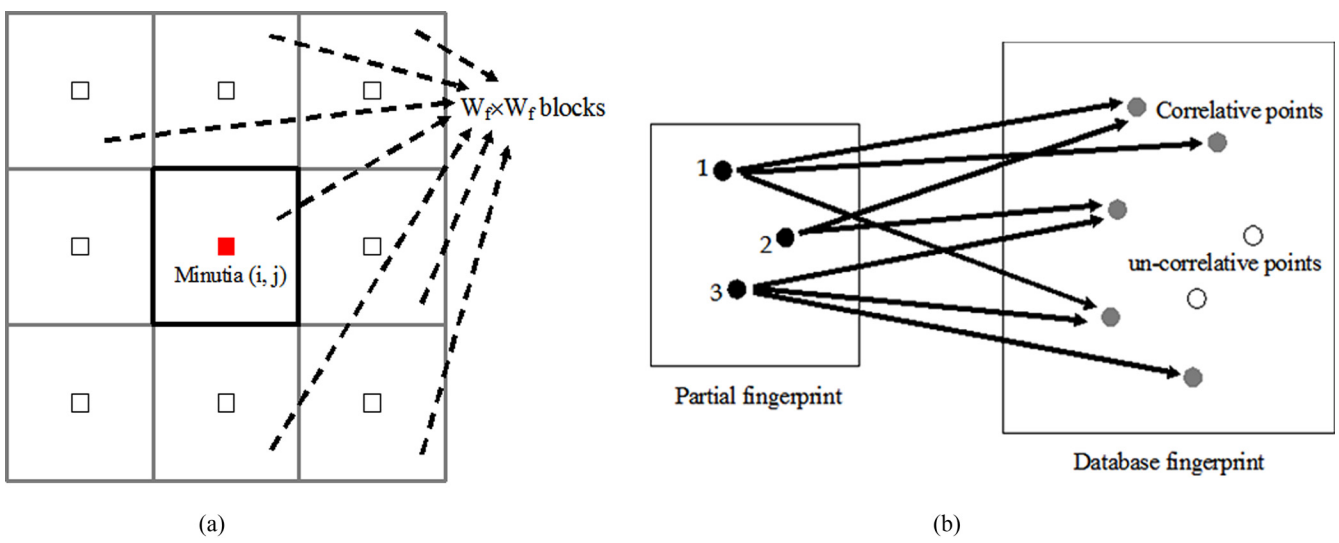


Figure 6. Computations regarding correlative points: (a) locating correlative points (b) correlative and uncorrelative points.

$$n=1 \rightarrow r_{1a}$$
$$=\frac{\sum_{i=1}^{9}(f_i(i_1,j_1)-\overline{f_1(i_1,j_1)})(f'_i(i_a,j_a)-\overline{f'_a(i_a,j_a)})}{\sqrt{\sum_{i=1}^{9}(f_i(i_1,j_1)-\overline{f_1(i_1,j_1)})^2}\sqrt{\sum_{i=1}^{9}(f'_i(i_a,j_a)-\overline{f'_a(i_a,j_a)})^2}},$$
$$n=2 \rightarrow r_{2a}$$
$$=\frac{\sum_{i=1}^{9}(f_i(i_2,j_2)-\overline{f_2(i_2,j_2)})(f'_i(i_a,j_a)-\overline{f'_a(i_a,j_a)})}{\sqrt{\sum_{i=1}^{9}(f_i(i_2,j_2)-\overline{f_2(i_2,j_2)})^2}\sqrt{\sum_{i=1}^{9}(f'_i(i_a,j_a)-\overline{f'_a(i_a,j_a)})^2}},$$
$$n=\ldots$$

where

$$\overline{f_n(i_n,j_n)}=\frac{1}{9}\sum_{i=1}^{9}f_i(i_n,j_n),$$
$$\overline{f'_a(i_a,j_a)}=\frac{1}{9}\sum_{i=1}^{9}f'_i(i_a,j_a). \quad (9)$$

From the above formulation, suppose $n$ be 1, the number of correlation coefficients we can get ($r_{11}$, $r_{12}$, $r_{13}$,…,$r_{1a}$) will be $a$. Now, let all minutiae, whose corresponding correlation coefficient is greater than $T_r$ (which is another predefined threshold) be recorded in a set $P_i$, $i=1$ to $n$, and simultaneously we let

$$Q=P_1\cup P_2\cup P_3\cup\cdots P_{n-1}\cup P_n, \quad (10)$$

where $Q$ is a collection of all correlative points, which are to be used in next step. Fig. 6(b) shows a schematic of correlative points and uncorrelative points. In this article, the size of our $w_f\times w_f$ blocks is $9\times 9$ and our $T_3$ and $T_r$ are 0.23 and 0.35, respectively, chosen as a compromise between speed and accuracy.

### *Finding Reference Points and Lines*

In the previous step, we have defined $P_1$, $P_2$, $P_3$,…,$P_n$, which are sets of correlative points corresponding to all minutiae points in the test image, having reasonably large correlation coefficients. Now we count how many points there are in each $P_i$ and let the counts be $S_i$, $i=1$ to $n$. Next, from $S_i$ we locate the largest two counts, and then we presume that the minutiae associated with these two largest counts are the ones having greatest correlation with the fingerprint database image in comparison. These two points are called reference points. The line segment connecting them is then a reference line for matching.

### *Computing Orientation Deflection Variation*

Since the test fingerprints of interest for comparison in this article are partial ones, the number of minutiae existing in one image is exceeding low. There are often only 5 or 6 of them. A new parameter, the coefficient of orientation deflection variation, is defined to enhance the capability for our system to recognize these partial fingerprints.

As in Figure 7(a), two reference points (minutiae 1 and 2) are shown. They denote the most correlated points in a test partial fingerprint image while being compared with a specific database fingerprint image. The two points define a reference line. Connecting this reference line to a third minutia point (minutia 3 in the figure) forms a triangle. We want to know how ridge orientation changes within this triangle, and then use this property as an additional feature in fingerprint matching.

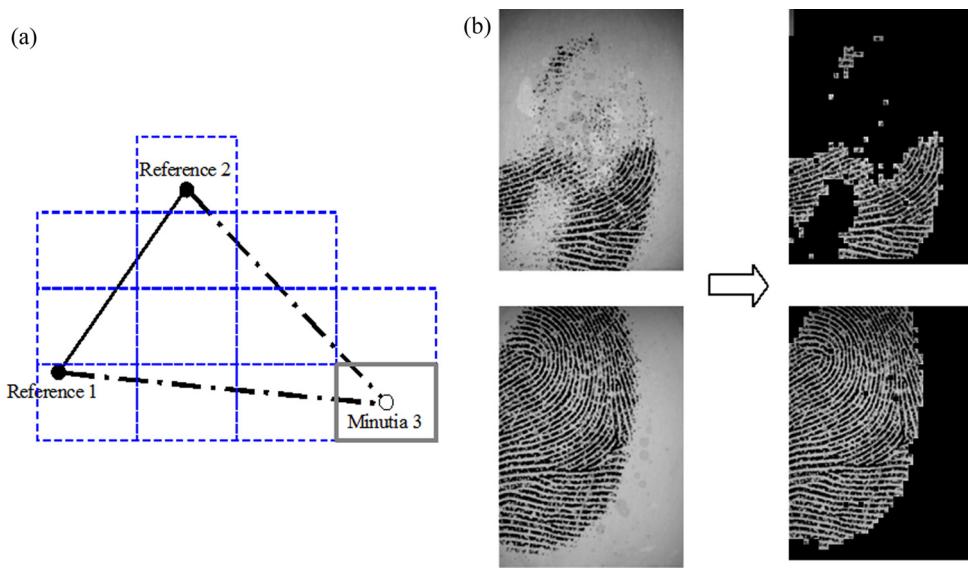


Figure 7. Developing a robust partial fingerprint matching scheme: (a) the triangular matching framework (b) removing the background.

First we obtain ridge orientation $O(i, j)$ at minutia 3 by the above stated method, with a block size of $w_z \times w_z$. Then, we also compute the orientations of the adjacent blocks, similarly sized as shown in Fig. 7(a), each covering at least some part of the triangular area. Assuming we have $n$ such blocks and hence $n$ orientations, i.e., $O(x_k,y_k)$, $k=1$ to $n$. The deviation of orientation is defined as

$$|O(x_k, y_k) - O(i, j)| = M_k \quad k = 1, 2, 3, \cdots n. \tag{11}$$

Subsequently, the coefficient of orientation deflection variation is defined as

$$\mathrm{CV}_M = \frac{S_M}{\overline{M}_M} \times 100\%, \tag{12}$$

where $S_M$ and $\overline{M}_M$ are, respectively, the standard deviation and the mean of the samples contained in the vector $M_k$.

From the above derivation, the coefficient of orientation deflection variation $\mathrm{CV}_M$ represents the degree of change associated with the ridge orientation within the triangular area measured with respect to that of minutia 3 because the definition starts from that point. We use it as an extra criterion for matching the fingerprints. However, if we pick another minutia point in Fig. 7(a) as the starting point, the $w_z \times w_z$ blocks for computing the orientation field will not be the same. We have to know that by permutation there are 36 cases. The above scheme we call the triangular matching scheme, and in this article we have $w_z = 9$.

## METHODOLOGY

It is generally accepted that the success of fingerprint matching depends heavily on the number of minutiae found in the fingerprint. So, it is difficult when a test fingerprint image contains only partial fingerprint where very few minutiae can be retrieved. When this is what we need to handle, every identified minutia must be used wisely and effectively.

As discussed previously, for matching an unknown fingerprint image with a database image, the processes normally include normalization and histogram equalization, then Gabor filtering and thinning. Afterwards, minutiae can be extracted, and the reference points and the reference line located. In this article, the proposed triangular matching scheme is used to assess the similarity between the two fingerprints.

In order to speed up the matching process, all fingerprint images can be preprocessed so that their foreground and background images are separated. This can be done by a coherence method proposed by Zhong et al.[26] Fig. 7(b) shows both a partial fingerprint image and a database fingerprint image, whose backgrounds have been removed.

After the fingerprint images are subjected to a series of preprocessing and minutiae extraction, Figure 8(a). Not all minutiae points are correlative points, as shown in Fig. 8(b). From all the correlative points we want to find some most correlated pairs as reference points. In this step, we use four

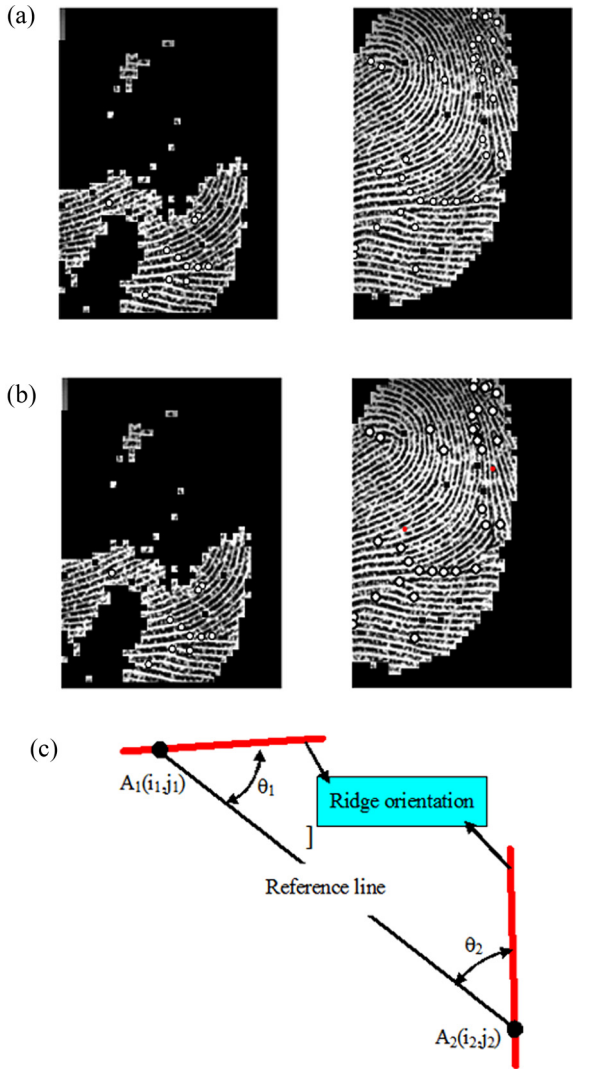


Figure 8. Minutiae and reference line related definitions: (a) extracting minutiae (squares are false minutiae); (b) detecting correlative points; (c) definitions of $\theta_1$ and $\theta_2$.

parameters to help determine the best candidates. They are $L$, the length of the reference line, $\theta$, the orientation difference between two reference points, $N$, the number of ridges passed by the reference line, and $\alpha$, the sum of the two angles $\theta_1$ and $\theta_2$ which are shown in Fig. 8(c).

The four parameters are computed for each pair of correlative points in the test (T) image and the database (D) image, arriving at two feature vectors $(L, \theta, N, \alpha)_\mathrm{T}$ and $(L, \theta, N, \alpha)_\mathrm{D}$. A matching reference line is said to be found when the absolute values of the difference between the two feature vectors is smaller than $(13, \pi/10, 3, \pi/10)$. These are again empirical threshold values. By this stringent criterion, Figure 9(a), where only two reference lines remain.

Once a suitable reference line is located to serve as the starting point for fingerprint verification, we apply the new triangular matching scheme as presented earlier. Not only is the coefficient of orientation deflection variation, $\mathrm{CV}_M$, used in this article as a matching criterion but we also employ the lengths, $l_1$, $l_2$, and the angles, $\theta_1$, $\theta_2$, as defined

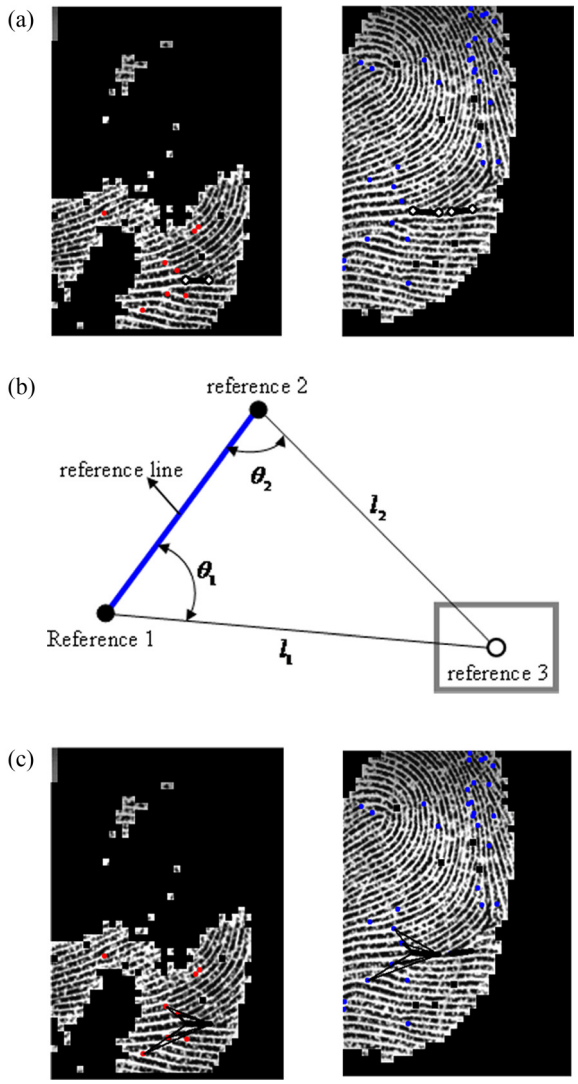


Figure 9. The triangular matching scheme, and its results: (a) finding reference lines as the starting point; (b) parameters used in the triangular matching scheme; (c) results from the triangular scheme.

in Fig. 9(b). Once more some threshold values are used to sieve off inappropriate results, i.e.,

$$|(l_1, l_2, \theta_1, \theta_2, \mathrm{CV}_M)_\mathrm{T} - (l_1, l_2, \theta_1, \theta_2, \mathrm{CV}_M)_\mathrm{D}| < (7, 7, \pi/12, \pi/12, 0.12).$$

As for the partial fingerprint example in Fig. 9, the final result is shown in Fig. 9(c), where only three triangles, which contain six points, pass our matching criteria.

## SAMPLES AND INDICATORS

In order to further verify the proposed method, 30 complete fingerprint samples with resolution of $388 \times 374$ are obtained from the database FVC2002 of DB1_B. There are unclear, blurred, or rotated samples, and there are actually ten different fingerprints in total. Partial fingerprints with the same size are produced from the original images by image editing software. Thus, we have 30 partial test fingerprint images and 30 database images.

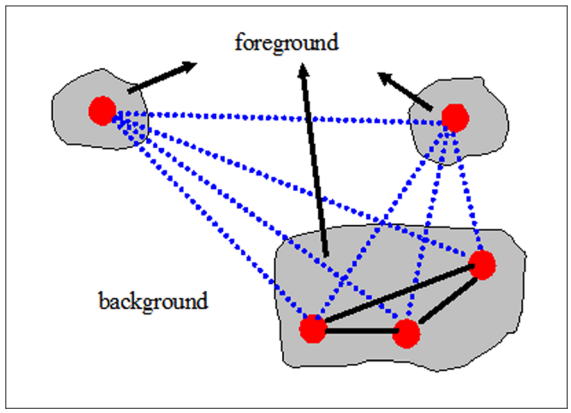


Figure 10. A fragmented partial fingerprint image.

In order to quantitatively evaluate the performance of the proposed fingerprint-matching scheme, some indicators need to be defined. This is true especially for our quest of partial fingerprint matching.

## INTEGRITY

First, a fragmentation factor $S_d$ is defined to help classify the partial fingerprint images. As shown in Figure 10, the foreground image of a partial fingerprint is usually seen as broken into separate parts. Let there be $n$ minutiae in this partial fingerprint. From these points a total of $\mathrm{N_L}$ lines can be drawn connecting all the minutiae. Then, the fragmentation factor $S_d$ is given as $\mathrm{N_B}/\mathrm{N_L}$, where $\mathrm{N_B}$ denotes the number of lines that pass through any part of the background. Clearly, the larger $S_d$, the more fragmented the partial fingerprint is. The opposite of $S_d$ is $S_a$, called the integrity factor of the fingerprint image, which is given by $S_a = 1 - S_d$. In our experiments, fingerprints with higher $S_a$ normally yield better matching results.

## FAR, FRR, ARM, AND FRM

Conventionally, there are indicators frequently used for evaluating the effectiveness of a biometric identification system. Among them are fault acceptance rate (FAR) and fault resistance rate (FRR). FAR is the error rate while matching different fingerprints, whereas FRR the error rate when matching the same fingerprints. Better identification systems should exhibit low FAR and FRR rates.

Besides FAR and FRR, we use two more indicators in our partial fingerprint matching experiments. We have accuracy rate of matching (ARM), which is the total accuracy rate, and fault rate of matching (FRM), which is the total failure rate of the matching experiment. The above four indicators are all used to show that the proposed scheme improves the success rate of partial fingerprint matching.

## RELATIVE COMPLETENESS

For partial fingerprint matching, there is a need to understand how incomplete a test fingerprint really is. Therefore,

**Table I.** Integrity factors of the ten sets of partial fingerprints used in the experiments.

| | a-1 | a-2 | a-3 | b-1 | b-2 | b-3 |
|---|---|---|---|---|---|---|
| Integrity ($S_a$) | 100% | 89.29% | 100% | 100% | 100% | 96.43% |
| | c-1 | c-2 | c-3 | d-1 | d-2 | d-3 |
| Integrity ($S_a$) | 100% | 100% | 85.45% | 100% | 100% | 100% |
| | e-1 | e-2 | e-3 | f-1 | f-2 | f-3 |
| Integrity ($S_a$) | 100% | 100% | 100% | 100% | 100% | 83.33% |
| | g-1 | g-2 | g-3 | h-1 | h-2 | h-3 |
| Integrity ($S_a$) | 100% | 92.73% | 100% | 100% | 100% | 96.43% |
| | i-1 | i-2 | i-3 | j-1 | j-2 | j-3 |
| Integrity ($S_a$) | 96.43% | 100% | 100% | 100% | 100% | 100% |

we define a parameter $S_f$, called relative completeness of the image, to indicate this property. $S_f$ is simply a ratio of the number of minutiae found in the partial fingerprint to that of a corresponding complete database fingerprint. Obviously, only when a successful matching is reached and can we compute this $S_f$.

## AVERAGE RELIABILITY

Before we explain the definition of the last indicator used in this article to measure the performance of matching, a factor K needs to be introduced. When $K=1$, it means that there are three matching points found in the fingerprint and from them a matching triangle is constructed. When $K=2$, we then have four matching points and two triangles, and so on. In this research, we normally require that at least $K=3$ to guarantee a successful matching. However, in Fig. 9(c), since we have six matching points and four matching triangles, $K=4$.

The average reliability of the matching, $S_c$, is then defined as such: When not a single reference line is found in the process, $S_c=0$. When there are separate reference lines, $S_c=40\%$. However, when reference lines can be connected to form matching triangles, we let $S_c=60\%$ as $K=1$, $S_c=80\%$ as $K=2$, and $S_c=100\%$ as $K=3$ or greater. This factor is used to discern whether a seemingly successful matching is really reliable.

**Table II.** Partial fingerprint matching results without considering the coefficient of orientation deflection variation $CV_M$.

| | $K=1$ | | $K=2$ | | $K=3$ | |
|---|---|---|---|---|---|---|
| Set | FRR | FAR | FRR | FAR | FRR | FAR |
| a | 11.11% | 96.30% | 11.11% | 92.59% | 22.22% | 77.78% |
| | (1/9) | (26/27) | (1/9) | (25/27) | (2/9) | (21/27) |
| b | 22.22% | 92.59% | 22.22% | 88.89% | 22.22% | 74.07% |
| | (2/9) | (25/27) | (2/9) | (24/27) | (2/9) | (20/27) |
| c | 22.22% | 85.19% | 22.22% | 77.78% | 33.33% | 66.67% |
| | (2/9) | (23/27) | (2/9) | (21/27) | (3/9) | (18/27) |
| d | 0% | 88.89% | 0% | 88.89% | 22.22% | 77.78% |
| | (0/9) | (24/27) | (0/9) | (24/27) | (2/9) | (21/27) |
| e | 0% | 92.59% | 0% | 85.19% | 0% | 66.67% |
| | (0/9) | (25/27) | (0/9) | (23/27) | (0/9) | (18/27) |
| f | 11.11% | 77.78% | 11.11% | 74.07% | 11.11% | 70.37% |
| | (1/9) | (21/27) | (1/9) | (20/27) | (1/9) | (19/27) |
| g | 0% | 100% | 0% | 100% | 11.11% | 81.48% |
| | (0/9) | (27/27) | (0/9) | (27/27) | (1/9) | (22/27) |
| h | 0% | 92.59% | 0% | 85.19% | 11.11% | 66.67% |
| | (0/9) | (25/27) | (0/9) | (23/27) | (1/9) | (18/27) |
| i | 22.22% | 88.89% | 22.22% | 88.89% | 22.22% | 74.07% |
| | (2/9) | (24/27) | (2/9) | (24/27) | (2/9) | (20/27) |
| j | 33.33% | 81.48% | 33.33% | 74.07% | 33.33% | 62.96% |
| | (3/9) | (22/27) | (3/9) | (20/27) | (3/9) | (17/27) |
| Total | 12.22% | 89.63% | 12.22% | 85.56% | 18.89% | 71.85% |
| | (11/90) | (242/270) | (11/90) | (231/270) | (17/90) | (194/270) |
| FRM | 253/360 = 70.28% | | 242/360 = 67.22% | | 211/360 = 58.61% | |
| ARM | 107/360 = 29.72% | | 118/360 = 32.78% | | 149/360 = 41.39% | |

**Table III.** Partial fingerprint matching results with considering the coefficient of orientation deflection variation $CV_M$.

| | $K=1$ | | $K=2$ | | $K=3$ | |
|---|---|---|---|---|---|---|
| Set | FRR | FAR | FRR | FAR | FRR | FAR |
| a | 11.11% | 81.48% | 11.11% | 55.56% | 33.33% | 22.22% |
| | (1/9) | (22/27) | (1/9) | (15/27) | (3/9) | (6/27) |
| b | 33.33% | 77.78% | 33.33% | 55.56% | 33.33% | 11.11% |
| | (3/9) | (21/27) | (3/9) | (15/27) | (3/9) | (3/27) |
| c | 22.22% | 70.37% | 33.33% | 48.15% | 33.33% | 40.74% |
| | (2/9) | (19/27) | (3/9) | (13/27) | (3/9) | (11/27) |
| d | 11.11% | 77.78% | 11.11% | 59.26% | 22.22% | 29.63% |
| | (1/9) | (21/27) | (1/9) | (16/27) | (2/9) | (8/27) |
| e | 0% | 81.48% | 11.11% | 48.15% | 11.11% | 22.22% |
| | (0/9) | (22/27) | (1/9) | (13/27) | (1/9) | (6/27) |
| f | 11.11% | 70.37% | 11.11% | 59.26% | 11.11% | 29.63% |
| | (1/9) | (19/27) | (1/9) | (16/27) | (1/9) | (8/27) |
| g | 0% | 74.07% | 22.22% | 62.96% | 33.33% | 37.04% |
| | (0/9) | (20/27) | (2/9) | (17/27) | (3/9) | (10/27) |
| h | 11.11% | 77.78% | 22.22% | 59.26% | 33.33% | 37.04% |
| | (1/9) | (21/27) | (2/9) | (16/27) | (3/9) | (10/27) |
| i | 22.22% | 85.19% | 33.33% | 62.96% | 33.33% | 33.33% |
| | (2/9) | (23/27) | (3/9) | (17/27) | (3/9) | (9/27) |
| j | 33.33% | 77.78% | 44.44% | 59.26% | 44.44% | 33.33% |
| | (3/9) | (21/27) | (4/9) | (16/27) | (4/9) | (9/27) |
| Total | 15.56% | 77.41% | 23.33% | 57.04% | 28.89% | 29.63% |
| | (14/90) | (209/270) | (21/90) | (154/270) | (26/90) | (80/270) |
| FRM | 223/360 = 61.94% | | 175/360 = 48.61% | | 106/360 = 29.44% | |
| ARM | 137/360 = 38.06% | | 185/360 = 51.39% | | 254/360 = 70.56% | |

## EXPERIMENT RESULTS

First, the integrity factors $S_a$ of the 30 partial fingerprint images we use in the experiment are listed in Table I. Subsequently, FAR and FRR values are obtained by letting K equal 1 and 2 and 3 in the experiments. For the FRR part, three images from the same database are treated as a set. Hence, nine comparisons are resulted for a set since there are three partial images and three database images. However, we have ten sets (Table I), so there are 90 comparisons in total. As for the FAR part, we pick one image from each set and compare it with all others in the 30 images. So, there will be $30 \times (10^{-1}) = 270$ comparisons. The results of the FAR, FRR, and FRM, ARM values are shown in Tables II and III, without and with making use of the coefficient of orientation deflection variation, $CV_M$, respectively.

From Tables II and III we find that by incorporating the proposed $CV_M$ as a matching criterion, accuracy is increased. As $K=3$, i.e., only five points are matched, we can have all error rates (FRR, FAR, FRM) reduced to around 29% and at the same time the total accuracy rate (ARM) increased to around 71%. For all successful comparisons, both in the FAR part and in the FRR part of the experiment, we also plot the distribution of the relative completeness factor $S_f$ and the average reliability factor $S_c$, as in Figures 11(a) and 11(b).

As $S_c$ (average reliability) is concerned, its distributions for both FAR and FRR experiments are reasonable. For the FRR part, a correct comparison means that the two fingerprint images do come from the same finger, and thus the average value of $S_c$ should be higher. On the contrary, a correct FAR result means that the two fingerprints in question come from different fingers. Therefore, its average $S_c$ value should be lower, though the counts are higher due to the greater number of experiments performed.

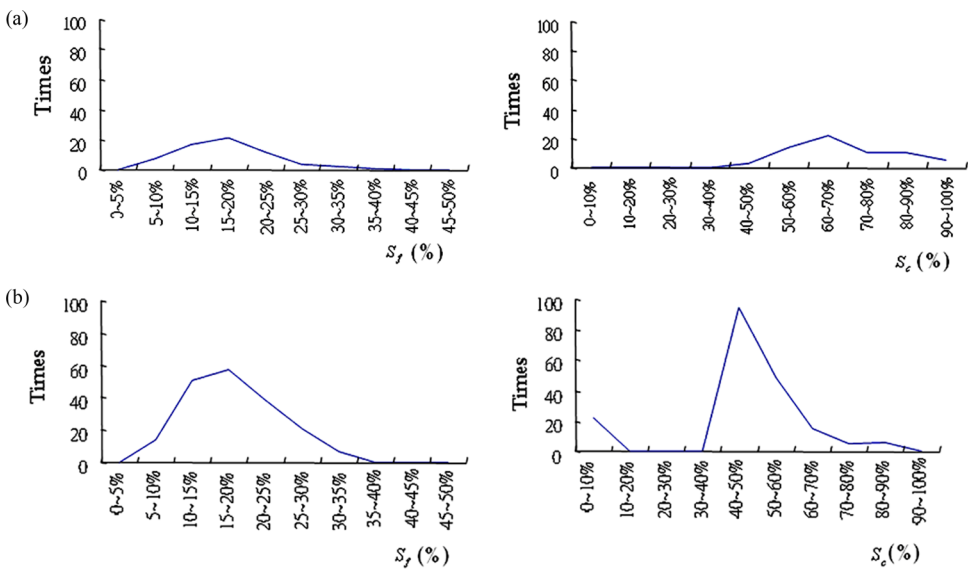


Figure 11. Distribution of relative completeness $S_f$ and average reliability $S_c$: (a) $S_f$ and $S_c$ distribution of the 90 FRR comparisons accomplished (b) $S_f$ and $S_c$ distribution of the 270 FAR comparisons accomplished.

Comparing the $S_c$ distributions with the $S_f$ (relative completeness) distributions, we find that there is not so much correlation between them. Although from Fig. 11, it is shown that the fingerprints we use in this article are indeed of low relative completeness, i.e., containing few minutiae; however, by the proposed triangular scheme coupled with the use of the coefficient of orientation deflection variation, it is still possible to achieve satisfactory matching results.

## SUMMARY

This article aims to contribute to a feasible scheme for the extraction and verification of the limited number of minutiae contained in a partial fingerprint. First, a refined minutiae extraction scheme is proposed to avoid the occurrence of so-called false minutiae points. Second, the mechanism for generating reference lines is revised to reduce matching errors. Third, a coefficient of orientation deflection variation is introduced, and when used with the new triangular matching scheme, it yields very satisfactory results. Finally, some indicators especially tailored for partial fingerprint matching are defined, which are useful in the evaluation of the effectiveness of the fingerprint matching system.

## ACKNOWLEDGMENTS

This research is partly supported by a research grant from the National Science Council of Taiwan, which is appreciated by the authors.

## REFERENCES

[1] E. R. Henry, *Classification and Uses of Finger Prints* (Routledge, London, 1900).
[2] A. K. Jain, L. Hong, and R. Bolle, "On-line fingerprint verification," IEEE Trans. Pattern Anal. Mach. Intell. **19**, 302–314 (1997).
[3] L. Hong, Y. Wan, and A. K. Jain, "Fingerprint image enhancement: Algorithm and performance evaluation," IEEE Trans. Pattern Anal. Mach. Intell. **20**, 777–789 (1998).
[4] T. Y. Zhang and C. Y. Suen, "A fast parallel algorithm for thinning digital patterns," Commun. ACM **27**, 236–239 (1984).
[5] R. C. Gonzalez and R. E. Woods, *Digital Image Processing*, 3rd ed. (Prentice-Hall, Englewood Cliffs, NJ, 2010).
[6] M. Kass and A. Witkin, "Analyzing oriented pattern," Comput. Vis. Graph. Image Process. **37**, 362–397 (1987).
[7] A. R. Rao, *A Taxonomy for Texture Description and Identification* (Springer-Verlag, New York, 1990).
[8] A. K. Jain, L. Hong, S. Pankanti, and R. Bolle, "An identity-authentication using fingerprints," Proc. IEEE **85**, 1365–1388 (1997).
[9] R. M. Stock and C. W. Swonger, "Development and evaluation of a reader of fingerprint minutiae," Technical Report No. CAL, XM-2478-X-l: 13-17, Cornell Aeronautical Laboratory (1969).
[10] K. Karu and A. K. Jain, "Fingerprint classification," Pattern Recogn. **17**, 389–404 (1996).
[11] A. K. Jain, S. Prabhakar, L. Hong, and S. Pankanti, "Filterbank-based fingerprint matching," IEEE Trans. Image Process. **9**, 846–859 (2000).
[12] B. Sherlock and D. Monro, "A model for interpreting fingerprint topology," Pattern Recogn. **26**, 1047–1055 (1993).
[13] P. Vizcaya and L. Gerhardt, "A nonlinear orientation model for global description of fingerprints," Pattern Recogn. **29**, 1221–1231 (1996).
[14] Z. Jie and G. Jinwei, "A model-based method for the computation of fingerprints' orientation field," IEEE Trans. Image Process. **13**, 821–835 (2004).
[15] F. H. Xiao and F. S. Peng, "Enhancement method for low quality fingerprint images," J. Data Acquis. Process. **20**, 440–443 (2005).
[16] I. Her, "Geometric transformations on the hexagonal grid," IEEE Trans. Image Process. **4**, 1213–1222 (1995).
[17] M. Tico and P. Kuosmanen, "An algorithm for fingerprint image post-processing," *Conference Record of the Thirty-Fourth Asilomar Conference on Signals, Systems and Computers 2* (Pacific Grove, CA 2000), pp. 1735–1739.
[18] P. L. Xi and T. Jie, "Image enhancement and minutiae matching algorithms in automated fingerprint identification system," J. Softw. **13**, 946–956 (2002).
[19] Z. Weiwei and W. Yangsheng, "Core-based structure matching algorithm of fingerprint verification," *Proc. 16th International Conference on Pattern Recognition 1* (Acad. Sinica, Beijing, China, 2002), pp. 70–74.
[20] L. Ning, Y. Yilong, and Z. Hongwei, "A fingerprint matching algorithm based on Delaunay triangulation net," *Fifth Int. Conf. on Computer and Information Technology* (Shanghai, China, 2005), pp. 591–595.
[21] N. K. Ratha, K. Karu, C. Shaoyun, and A. K. Jain, "A real-time matching system for large fingerprint databases," IEEE Trans. Pattern Anal. Mach. Intell. **18**, 799–813 (1996).
[22] L. Chaoqiang, X. Tao, and L. Hui, "A hierarchical Hough transform for fingerprint matching," *Proc. 1st Int. Conf. on Bioinformatics and its Applications* (Springer-Verlag, Berlin/Heidelberg, 2004), pp. 373–379.
[23] Q. Jin, S. Zhongchao, Z. Xuying, and W. Yangsheng, "A novel fingerprint matching method based on the Hough transform without quantization of the Hough space," *Proc. Third Int. Conf. on Image and Graphics* (Hong Kong, China, 2004), pp. 262–265.
[24] G. Fang, S. Srihari, Srinivasan, and P. Phatak, "Use of ridge points in partial fingerprint matching," Proc. SPIE Biometric Technology for Human Identification, Orlando, FL, April 2007.
[25] Z. Hou, W. Y. Yau, and Y. Wang, "A review on fingerprint orientation estimation," Sec. Commun. Networks **4**, 591–599 (2011).
[26] C. S. Zhong, S. W. Yang, Q. Jin, and X. Ke, "A new segmentation algorithm for low quality fingerprint image," *Proc. Third Int. Conf. on Image and Graphics*, (Hong Kong, China, 2004), pp. 314–317.